Article ID: 1006-8775(2016) 02-0200-08

ESTIMATION OF OBSERVATION IMPACT WITH AN ENSEMBLE SENSITIVITY METHOD

LI Hong (李 泓)[1,2], WANG Qin (王 琴)[3]
(1. Shanghai Typhoon Institute of CMA, Shanghai 200030 China; 2. Key Laboratory of Numerical Modeling for Tropical Cyclone of CMA, Shanghai 200030 China; 3. Shanghai Marine Meteorological Center, Shanghai 201300)

Abstract: The ensemble based forecast sensitivity to observation method by Liu and Kalnay is applied to the SPEEDY-LETKF system to estimate the observation impact of three types of simulated observations. The estimation results show that all types of observations have positive impact on short-range forecast. The largest impact in Northern Hemisphere is produced by rawinsondes, followed by satellite retrieved profiles and cloud drift wind data, which in Southern Hemisphere is produced by satellite retrieved profiles, rawinsondes and cloud drift wind data. Satellite retrieved profiles influence more on the Southern Hemisphere than on the Northern Hemisphere due to few observations from rawinsondes in the Southern Hemisphere. At the level of 200 to 300 hPa, the largest impact is attributed to wind observations from rawinsondes and cloud drift wind.

Key words: observation impact; EFSO; LETKF
CLC number: P435 **Document code:** A
doi: 10.16555/j.1006-8775.2016.02.010

1 INTRODUCTION

As the number of observations has rapidly increased, especially that of satellite observations, it has become necessary to assess the impact of each observation since it is not clear that these observations are always assimilated properly and beneficial to model forecast. Therefore, the ability of estimating observation impact is essential for improving model performance and future observing system design. The traditional approach to estimate observation impact is Observing System Experiments (OSEs) by carrying out analyses and forecasts with and without assimilating a specified data (Bouttier and Kelly[1]; Li et al.[2]; Yang et al.[3]). However, carrying out OSEs with various observation datasets is computationally very expensive. Langland and Baker [4] developed an adjoint-based Forecast Sensitivity to Observation (FSO) method which allows the impact of each individual observation to be estimated once and then summed up according to any desired subset, such as instrument type, observed variable or location. Due to its low cost, this FSO method has been widely used in various operational systems (Zhu and Gelaro[5]; Cardinali[6]). However, it requires the adjoint operators for both forecast model and data assimilation system. As an alternative, Liu and Kalnay [7] and Li et al.[8] proposed an ensemble-based FSO (EFSO) method without the adjoint model in an ensemble Kalman filter. This method was initially tested in the Lorenz 40 variables model, and Wang et. al. [9] successfully applied it on a simplified AGCM model and estimated the impact of simulated rawinsonde data.

In this study, we extend the work of Wang et. al.[9] to add satellite observations, including satellite retrieved profiles and cloud drift wind, to simulate more realistic observing network and to further evaluate the ability of EFSO to assess observation impact for various data.

2 METHODOLOGY

2.1 *The LETKF*

We use the local ensemble transform Kalman filter (LETKF, see Hunt et al.[10]) to assimilate observations. The LETKF belongs to the family of ensemble Kalman filter (EnKF). It has two steps; Eq.(1) updates the ensemble mean, and then Eq. (2) updates the ensemble perturbations by transforming the forecast perturbations $\boldsymbol{X}^b$ through a transform matrix $[(\boldsymbol{K}-1)\widetilde{\mathbf{P}}^a]^{1/2}$.

$$\bar{\mathbf{x}}^a=\bar{\mathbf{x}}^b+\boldsymbol{X}^b\widetilde{\mathbf{P}}^{\mathbf{a}}(\mathbf{H}\mathbf{X}^{\mathbf{b}})^{\mathbf{T}}\mathbf{R}^{-1}[\mathbf{y}^{\mathbf{o}}-h(\bar{\mathbf{x}}^b)] \quad (1)$$

$$\boldsymbol{X}^a=\boldsymbol{X}^b[(K-1)\widetilde{\mathbf{P}}^a]^{1/2} \quad (2)$$

here y^o stands for observations and R the observation error covariance (a diagonal matrix containing only the observation error standard deviations). K is the number of ensembles, h the nonlinear observation operator and H its linear matrix. $\boldsymbol{X}^a$, $\boldsymbol{X}^b$ are the analysis and forecast

Received 2015-09-06; **Revised** 2016-01-29; **Accepted** 2016-04-15
Foundation item: National Natural Science Foundation of China (41575107,40975067); 973 Program (2013CB430305); Project of Shanghai Meteorological Bureau (YJ201401) ; National Programme on Global Change and Air-Sea Interaction (GASI-IPOVAI-04)
Biography: LI Hong, Ph.D., associate professor, primarily undertaking research on data assimilation and numerical modeling.
Corresponding author: LI Hong, e-mail: lih@mail.typhoon.gov.cn

ensemble perturbations, respectively. $\widetilde{\mathbf{P}}^a$, the analysis error covariance in ensemble space, is given by

$$\widetilde{\mathbf{P}}^a=[(K-1)\mathbf{I}+(\mathbf{HX}^b)^T\mathbf{R}^{-1}(\mathbf{HX}^b)]^{-1} \quad (3)$$

which has a dimension of K by K, much smaller than either the dimension of the model or the number of observations. Thus, LETKF performs the matrix inverse in the space spanned by background ensembles, which greatly reduces the computational cost.

2.2 *EFSO method*

Following Liu and Kalnay [7] and Wang et al.[9], we define the cost function to measure the forecast error reduction at time t due to assimilating observations at time 0.

$$J=\frac{1}{2}(\mathbf{e}_{t|0}^T\mathbf{C}\mathbf{e}_{t|0}-\mathbf{e}_{t|-6}^T\mathbf{C}\mathbf{e}_{t|-6})=\frac{1}{2}(\mathbf{e}_{t|0}+\mathbf{e}_{t|-6})\,\mathbf{C}(\mathbf{e}_{t|0}-\mathbf{e}_{t|-6}) \quad (4)$$

As in Fig.1, $\mathbf{e}_{t|0}=\mathbf{x}_{t|0}^f-\mathbf{x}_t$ is the perceived error of the forecast $\mathbf{x}_{t|0}^f$ at time t that starts from the analysis at time 0 and $\mathbf{x}_t$ is the 'true' state at time t. $\mathbf{e}_{t|-6}=\mathbf{x}_{t|-6}^f-\mathbf{x}_t$ is the corresponding error of the forecast $\mathbf{x}_{t|-6}^f$ starting from the analysis at time −6 h. The difference between the error $(e_{t|0}-e_{t|-6})$ is due solely to the observations $\mathbf{y}_0^o$ assimilated at time 0, therefore J is generally negative since the error $\mathbf{e}_{t|0}$ is usually less than the error $\mathbf{e}_{t|-6}$. In Eq.(1) C is a matrix of energy weighting coefficients to account for different units and magnitudes for different model variables.

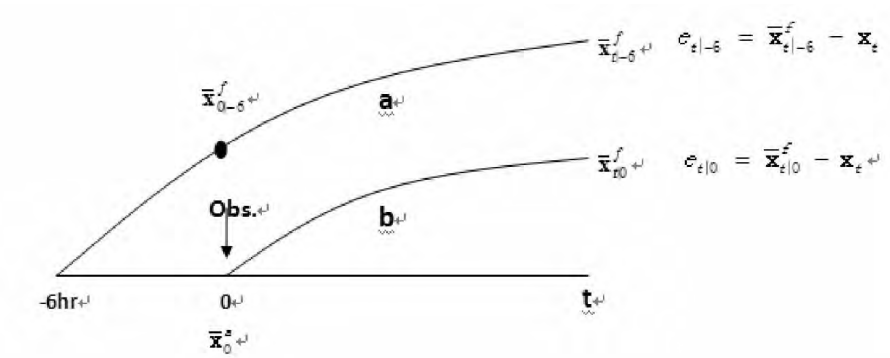

Figure 1. A schematic of the impact of observations assimilated at time 0 on forecast at time t: observations assimilated at time 0 creating initial conditions for a new trajectory $\bar{\mathbf{x}}_{t|0}^f$, which has forecast error $e_{t|0}$ and the old trajectory starting from time −6 h $\bar{\mathbf{x}}_{t|-6}^f$, which has forecast error $e_{t|-6}$. The error difference $(e_{t|0}-e_{t|-6})$ is due solely to the assimilation of observations at time 0.

By substituting the definitions of $\mathbf{e}_{t|0}$ and $\mathbf{e}_{t|-6}$ into Eq.(4), the cost function can be rewritten as:

$$J=\frac{1}{2}(2\mathbf{e}_{t|-6}+\mathbf{x}_{t|0}^f-\mathbf{x}_{t|-6}^f)^T\mathbf{C}(\mathbf{x}_{t|0}^f-\mathbf{x}_{t|-6}^f) \quad (5)$$

Using the LETKF formula, $(\mathbf{x}_{t|0}^f-\mathbf{x}_{t|-6}^f)$ is rewritten as a function of the observation increment $\mathbf{v}_0=\mathbf{y}_0^o-h(\mathbf{x}_{0|-6}^b)$ at time 0

$$\mathbf{x}_{t|0}^f-\mathbf{x}_{t|-6}^f\cong\mathbf{X}_{t|-6}^f\widetilde{\mathbf{K}}_0\mathbf{v}_0 \quad (6)$$

where $\mathbf{X}_{t|-6}^f$ is forecast perturbation at time t starting from time −6 h, $\widetilde{\mathbf{K}}_0$ is the Kalman gain matrix at time 0 in the subspace spanned by the forecast ensemble perturbation and has been calculated in the LETKF at time 0. For more detailed derivation of the EFSO method, refer to Liu and Kalnay [7] and Li et al.[8].

Therefore,

$$J=(\mathbf{e}_{t|-6}+\frac{1}{2}\mathbf{X}_{t|-6}^f\widetilde{\mathbf{K}}_0\mathbf{v}_0)^T\mathbf{C}\mathbf{X}_{t|-6}^f\widetilde{\mathbf{K}}_0\mathbf{v}_0) \quad (7)$$

or

$$J=\langle\mathbf{v}_0,\widetilde{\mathbf{K}}_0^T\mathbf{X}_{t|-6}^{fT}\mathbf{C}[\mathbf{e}_{t|-6}+\frac{1}{2}\mathbf{X}_{t|-6}^f\widetilde{\mathbf{K}}_0\mathbf{v}_0]\rangle \quad (8)$$

According to Eq.(8), the impact of each individual observation i will be calculated by:

$$J_i=v_{0(i)}\cdot[(\mathbf{X}_{t|-6}^f\widetilde{\mathbf{K}}_0)^{\mathrm{T}}\cdot\mathbf{C}\cdot(\mathbf{e}_{t|-6}+0.5\mathbf{X}_{t|-6}^f\widetilde{\mathbf{K}}_0v_0]_{(i)} \quad (9)$$

We say the observation i is beneficial (harmful) if the J_i is negative (positive), since it implies forecast error reduction (increment). The impact of a specific subset is simply the sum of all the individual impacts in the subset, and the sum of all the observational impact is equivalent to the cost function in Eq.(8).

Following Wang et al.[9], the norm operator C is defined as a coefficients matrix of dry-air kinetic energy equation E, where

$$E=\frac{1}{2}(u^2+v^2)+\frac{c_p}{T_r}T^2+\frac{R_d.T_r}{P_r^2}P_s^2 \quad (10)$$

where c_p=1005.7*J*.kg $^{-1}$.*K* $^{-1}$, T_r=270*K*, R_d =287*J*.kg $^{-1}$, P_r=10^5*Pa*.

3 EXPERIMENTAL DESIGN

As in Wang et al.[9], we use the Simplified Parameterizations primitivE Equation DYnamics (SPEEDY) model with resolution T30L7, a simplified atmospheric model which has been widely used in various research

studies (Danforth et al.[11]; Li et al.[12]; Amezcua et al.[13]). First, we assume a perfect model where a nature run is generated by integrating the SPEEDY model from 0000 UTC 1 January, 1987 until 1800 UTC 15 February, 1987. The observations are simulated by adding normally distributed random noise to the nature run. In addition to the rawinsonde data used in Wang et al.[9], two more types of data are included: satellite retrieved atmospheric profiles and cloud drift wind data. The observation errors are 1 m/s for u, v wind, 1 K for T, 10^{-4} kg/kg for q and 1 hPa for p_s with rawinsondes; 2 K for T, 2×10^{-4} kg/kg for q with satellite retrieved atmospheric profiles; and 3 m/s for u, v with cloud drift wind. The error values are specified to take account of the qualities of three types of real data, as well as the fact that satellite retrievals are with the strong error correlations and their error standard deviations need to be amplified[2] since we have ignored the error correlation terms in the observation error covariance matrix R (R is a diagonal matrix in the LETKF formula). The global distribution of the three types of data is shown in Fig.2. The network of rawinsonde is simulated with the real operational rawinsonde stations. Satellite retrievals are distributed regularly on every model grid point and all 7 vertical levels. Cloud drift wind data are available regularly on every half-grid shifted points at low and middle latitudes and in the upper levels only (Fig.6). These data are assimilated four times daily at analysis time 0000 UTC, 0600 UTC, 1200 UTC and 1800 UTC from 1 January to 15 February, while the impact assess experiments are performed only in the last half month allowing for the first month as a 'spin-up' period. The cost function in this study is defined as the difference between 06 h and 12 h forecast error ($e_{6|0}-e_{6|-6}$) which is due entirely to the assimilation of observations at the analysis time.

4 OBSERVATION IMPACT RESULTS

4.1 *Global distribution of observation impact*

Figure 2 shows the global distribution of observation impact. The impact value is averaged for all the observed variables and vertical levels at each observation location. For rawinsondes (Fig.2b), data over ocean is sparse and the individual profile has large impact and contributes to reducing forecast errors (negative value). In contrast, data over land is dense and the impact from individual profiles is smaller and some of them have

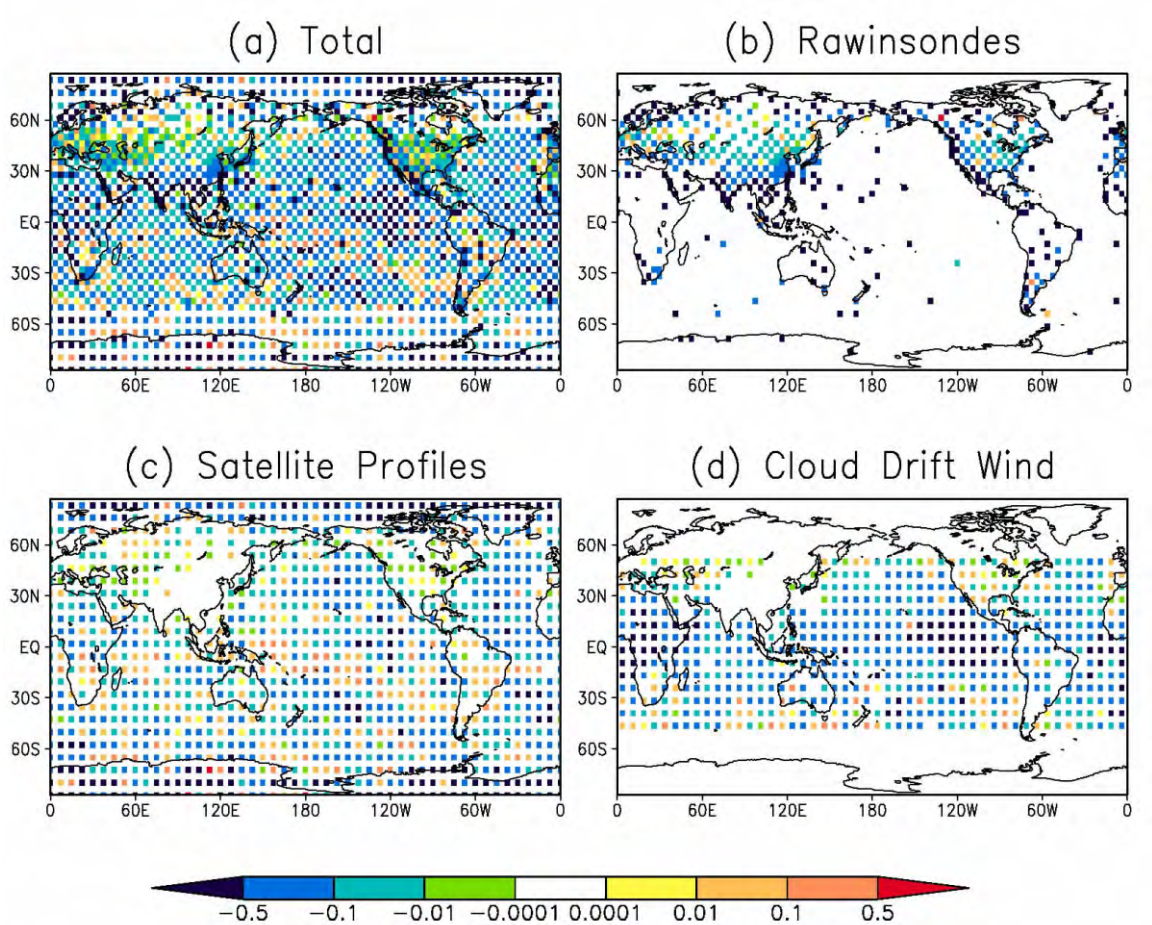

Figure 2. Global distribution of observation impact (Unit: J/kg) averaged for the period from 0000 UTC, February 1 to 1800 UTC, February 15. Green (yellow) dots represent reduction (increase) in forecast error. The four panels are for (a) all the observations, (b) rawinsondes , (c) satellite retrieved profiles and (d) cloud drift wind, respectively.

negative contribution to forecast (positive value). For satellite retrieved profiles, the impact of individual profiles is relatively smaller and more mixed contribution than that of rawinsonde, the largest contribution is found in polar region. For cloud drift wind, though many observations degrading forecast, most observations in the tropics improve forecast.

4.2 *Grouping observation impact for specific subsets*

It is convenient to group the observation impact according to any arbitrary subset, such as instrument type, observed variable or geographic location, since the grouped impact is simply the sum of all individual impacts in the subset. Below we will consider some subsets of our interest.

We first group the impacts by Hemisphere. The summed hemispheric observation impact for Southern Hemisphere is smaller than that for Northern Hemisphere. However, the impact per observation is similar in the two hemispheres (Fig.3). In this discussion, the term "impact per observation" is the summed impact of a set of observations divided by the number of observations in the set of data.

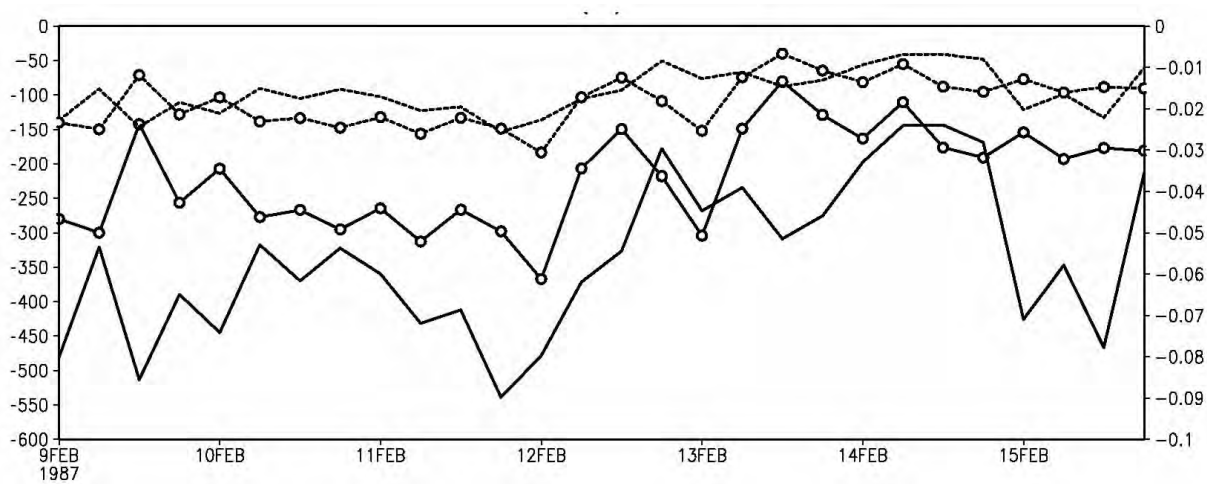

Figure 3. Time series of observation impact partitioned by different hemispheres (Unit: J/kg). Left *y*-coordinate is for summed impact of Northern (solid line) and Southern (dot-solid line) Hemisphere, right *y*-coordinate is for impact per observation of Northern (dashed line) and Southern (dot-dashed line) Hemisphere.

We then group the impacts by instrument type and Hemisphere. Overall, all types of observations are beneficial to forecast in both hemispheres, as shown in Fig.4. In Northern Hemisphere, the largest impact is provided by rawinsondes, followed by satellite retrieved profiles and cloud drift wind. In Southern Hemisphere, the largest impact is from satellite retrieved profiles, followed by rawinsondes and cloud drift wind. The largest impact of rawinsonde in Northern Hemisphere is probably due to the largest number of rawinsondes (Fig.4) and most of them are individually beneficial to forecast (Fig.2b).

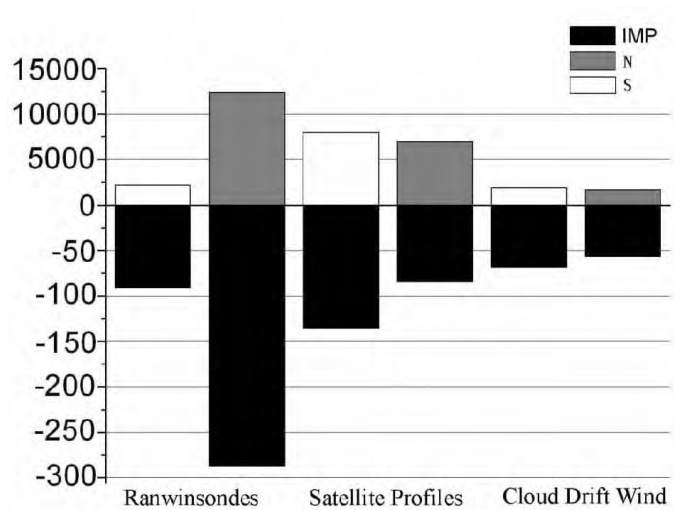

Figure 4. Summed observation impact partitioned by instrument type and hemisphere (black bars, Unit: J/kg) and the number of observations (white bars for Southern Hemisphere, grey bars for Northern Hemisphere) for each instrument type.

Next, we group impacts by vertical level (Fig.5). The impacts increase with height, and reach maximum at the level of 200 to 300 hPa. This is probably due to a large number of observations there and the biggest background error in wind field (see discussion below).

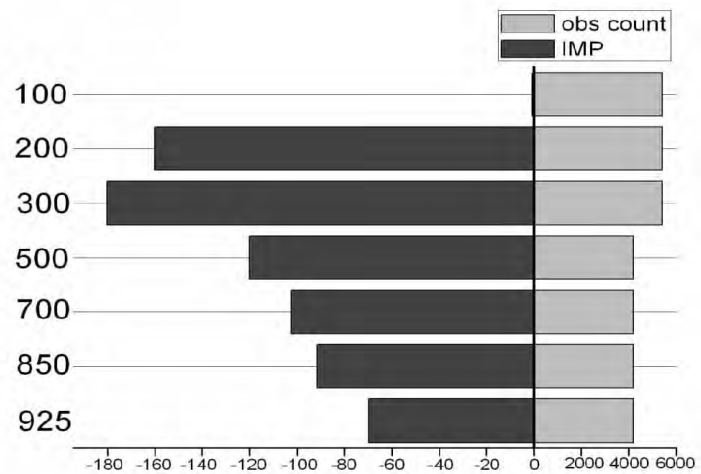

Figure 5. Summed observation impact partitioned by vertical level (black bars, Unit: J/kg) and the number of observations (grey bars).

The summed observation impacts partitioned by vertical level, observed variable and instrument type are shown in Fig.6. For rawinsondes, the largest impact is in the upper level (except 100 hPa), mainly contributed by u, v observations; The large u, v impacts of rawinsonde and cloud drift wind are both around 200 hPa~300 hPa, which is consistent with the biggest background error of u, v variables (Fig.7a, b), indicating

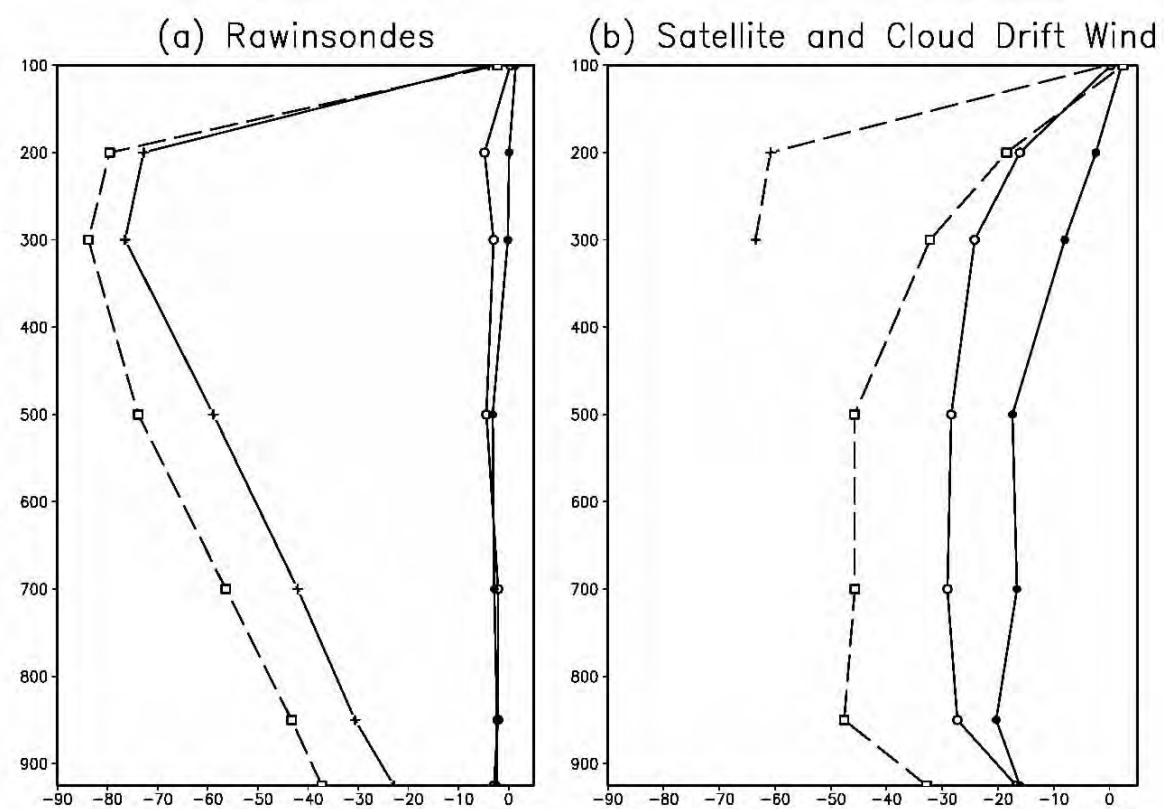

Figure 6. Vertical distribution of (a) observed variables u, v (+), T (○), q (●) impact, and the summed impact of u, v, T, q (□) for rawinsonde; (b) observed variables T (○), q (●), and the summed impact of T, q (□) for satellite retrievals; u, v (+) impact for cloud drift wind (Unit: J/kg).

observations are more beneficial where background fields are of worse quality; On the other hand, since the observation error of u, v is 1 m/s for rawinsonde and 3 m/s for cloud drift wind, the u, v impact of rawinsonde is larger than that of cloud drift wind; For satellite retrievals, the impact of q is smaller than that of T, and distributes mostly below 500 hPa, consistent with the large humidity background error in the lower levels. All of the results above indicate that the observation impact depends not only on the observations (quality, type, distribution, etc) but also on the model background. In general, the worse the background is (and/or the more and better observation is), the larger the observation impact will be. Of course, the background field itself is determined by assimilation system and forecast model, which is out of the scope of this study.

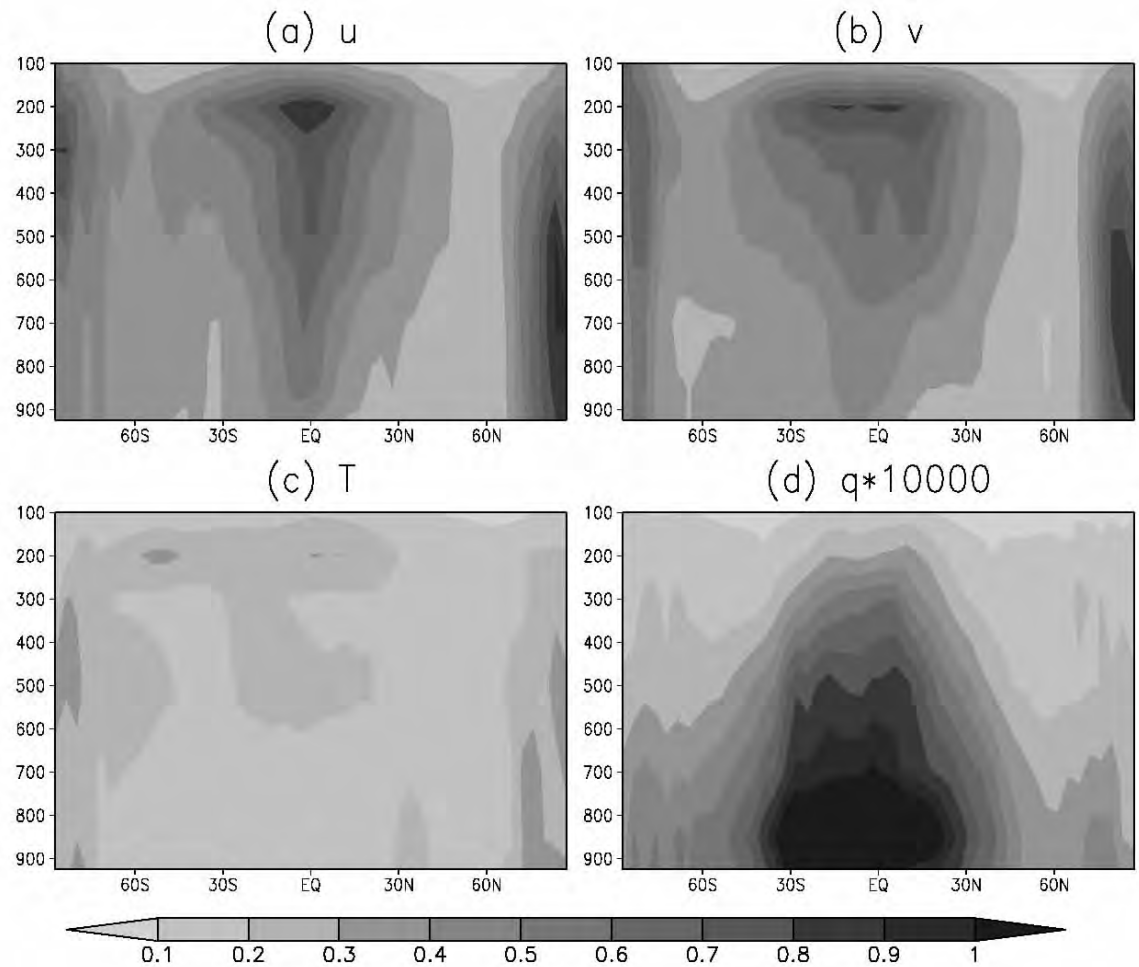

Figure 7. Background error for (a) u (m/s), (b) v (unit: m/s), (c) T (unit: K), (d) q (kg/kg) averaged over the experimental period.

Finally we compare the impacts of two types of satellite observation (Fig.8). For retrieved profiles, the largest impact is found in the polar region. This is easy to understand because there is not any other observation type in the poles therefore the retrieved T and q profiles have the sole impact on forecast. In contrast, the impact of cloud drift wind is largest in tropics, associated with the biggest background error of upper level wind there (Fig.7a, b). In general, the impact of cloud drift wind at every latitude is larger than that of satellite retrievals while its total impact is smaller (Fig.4) since these data covers only three upper levels (Fig.6) and no data at high latitudes (Fig.2d).

5 CONCLUSIONS

In this study, the ensemble sensitivity method [7] with the SPEEDY-LETKF system is applied to estimate the impact of simulated observation on forecast. This ensemble-based FSO (EFSO) method inherits the advantage of FSO which allows observation impact to be calculated once and be summed for any subset of observations, but without using an adjoint model. The simulated data include rawindsonde, satellite retrieved atmospheric profile and cloud drift wind.

All of the individual impacts of each observation are calculated by Eq.(9), the total impact of the global

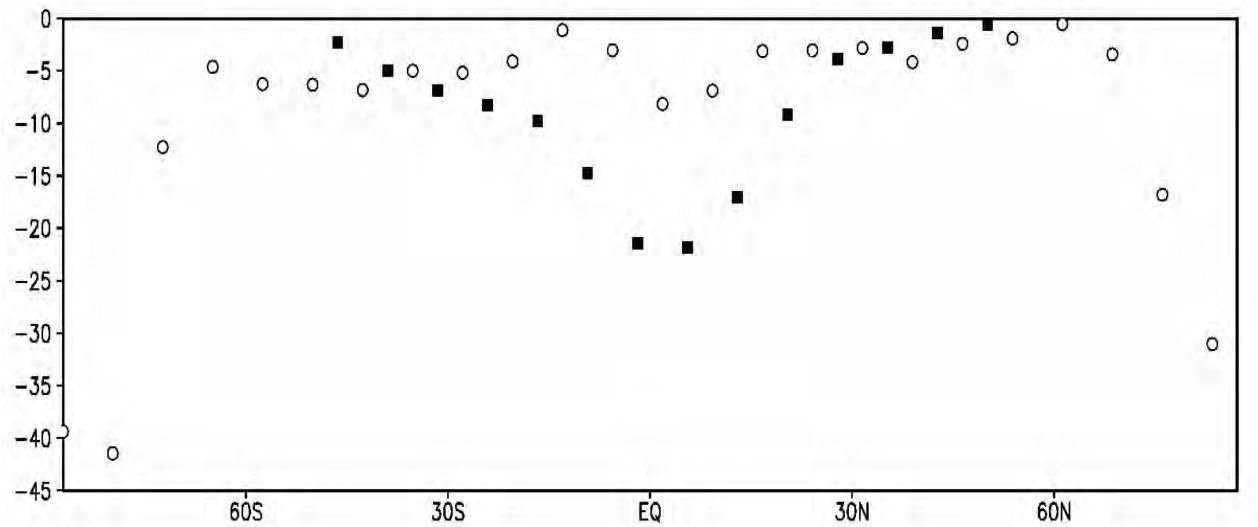

Figure 8. Summed observation impact partitioned by instrument type and latitude for satellite retrieved profiles (white cycle) and cloud drift wind (black square). Unit: J/kg.

observation is the sum of all the individual impacts. The impacts are then grouped by instrument type, geographic region, observed variable, vertical level or a combination of these categories. Our results show: (1) Individual impact of a rawinsonde profile is relatively larger and more beneficial to forecast than that of satellite observations; (2) All types of observations have an overall positive contribution to reducing forecast errors. Rawinsonde has the largest contribution in Northern Hemisphere. In Southern Hemisphere, the largest impact is produced by satellite retrieved profiles followed by rawinsondes and cloud drift wind. (3) Vertically, the largest impact occurs at the level of 200 to 300 hPa. (4) The impact of u, v from rawinsonde is much larger than that of T and q; the impact of q from satellite retrievals is smaller than that of T, and distributes mostly below 500 hPa. (5) Satellite retrievals contribute more in the polar region while the impact of cloud drift wind is largest in tropics.

The observation impact is not only determined by the observations but also strongly associated with the background field whose quality depends on both assimilation system and forecast model. In this study, the SPPEDY-LETKF system has large background error in the 200 to 300 hPa wind field therefore the u, v impacts (of both rawinsondes and cloud drift wind) at the upper level are larger than the other variables. In general, the worse background and/or better observation produce larger and positive observation impact.

This study further proves the ability of EFSO to assess observation impact efficiently for various data and to obtain reasonable impact results. It should be noted that our results shown here are based on simulated observations and the SPPEDY-LETKF system. With real observations and other ENKF systems, the observation impact will be different because all the three factors (observations, assimilation system and forecast model) which affect the estimation results could be substantially different.

REFERENCES:

[1] BOUTTIER F, KELLY G. Observing-system experiments in the ECMWF 4D-Var data assimilation system [J]. Quart J Roy Meteorol Soc, 2001, 127: 1 469-1 488.

[2] LI H, LIU J, FERTIG E. Improved analysis and forecasts with AIRS temperature retrievals using the local ensemble transform Kalman filter [J]. J Trop Meteorol, 2011, 17(1): 43-49.

[3] YANG Yin-ming, DU Ming-bin, ZHANG Jie. FY-3A satellite microwave data assimilation experiment in tropical cyclone forecast [J]. J Trop Meteorol, 2013, 19 (3): 297-304.

[4] LANGLAND R H, BAKER N L. Estimation of observation impact using the NRL atmospheric variational data assimilation adjoint system [J]. Tellus, 2004, 56: 189-201.

[5] ZHU Y, GELARO R. Observation sensitivity calculations using the adjoint of the gridpoint statistical interpolation (GSI) analysis system [J]. Mon Wea Rev, 2008, 136: 335-350.

[6] CARDINALI, C. Monitoring the observation impact on the short-range forecast [J]. Quart J Roy Meteorol Soc, 2009, 135: 239-250.

[7] LIU J, KALNAY E. Estimating observation impact without adjoint model in an ensemble Kalman filter [J]. Quart J Meteorol Soc, 2008, 134(634): 1 327-1 335.

[8] LI H, LIU J, KALNAY E. Letter to the editor Correction of "Estimating observation impact without adjoint model in an ensemble Kalman filter" [J]. Quart J Roy Meteorol Soc, 2010, 136: 1 652-1 654.

[9] WANG Qin, WANG Pan-xing, LI Hong. Ensemble Based Estimation of Observation Impact—a Simplified Parameterization AGCM Perfect Model Experiments [J]. Chin J Atmos Sci, 2010, 34(4): 793-801 (in Chinese).

[10] HUNT B R, KOSTELICH E J, SZUNYOGH I. Efficient data assimilation for spatiotemporal chaos: a local ensemble transform Kalman filter [J]. Physica D: Nonlinear phenomena, 2007, 230: 112-126.
[11] DANFORTH C M, KALNAY E, MIYOSHI T. Estimating and correcting global weather model error [J]. Mon Wea Rev, 2007, 135(2): 281-299.
[12] LI H, KALNAY E , MIYOSHI T , et al. Accounting for model errors in ensemble data assimilation [J]. Mon Wea Rev, 2009, 137: 3 407-3 419.
[13] AMEZCUA J, KALNAY E, WILLIAMS P D. The Effects of the RAW Filter on the Climatology and Forecast Skill of the SPEEDY Model [J]. Mon Wea Rev, 2011, 139: 608-619.

Citation: LI Hong and WANG Qin. Estimation of observation impact with an ensemble sensitivity method [J]. J Trop Meteorol, 2016, 22(2): 200-207.